

## Calibration and stability of the High Resolution Fly's Eye detector

B. F. Jones, J. N. Matthews, S. A. Moore, and S. B. Thomas  
for the High Resolution Fly's Eye Collaboration

High Energy Astrophysics Institute and The Department of Physics, University of Utah

**Abstract.** An *in situ* statistical method of calibration for the High Resolution Fly's Eye detector has been developed and is in routine use. The resulting calibration of the photomultiplier tubes and the long term stability of the detector are discussed.

### 1 Introduction

The goal of the High Resolution Fly's Eye (HiRes) project is to study cosmic rays of the highest energies. An ultra-high energy cosmic ray entering the earth's atmosphere collides with atmospheric nuclei triggering the development of an Extensive Air Shower (EAS). The EAS emits fluorescence light as it develops. HiRes uses the air fluorescence signal to measure properties of the primary cosmic ray particle.

The fundamental detector elements in HiRes are 16,000 photomultiplier tubes (PMTs) located at two nearby experimental sites in Utah. The light from an EAS is collected by large mirrors and focused into cameras consisting of 256 PMTs. Routine monitoring and calibration of the PMTs and associated electronics is crucial to the proper interpretation of the data.

### 2 Calibration Hardware Systems

Two systems are currently employed by HiRes to monitor the night-to-night and month-to-month stability of the PMTs and electronics. The first system simultaneously illuminates all of the PMT cameras at one site with light distributed from a single 355 nm YAG laser. This system is routinely operated at the beginning and end of each night. The light from the YAG laser is transported by quartz optical fibers to the center of each mirror where it is attenuated and diffused to uniformly illuminate the PMTs. Tuning of the atten-

uator/diffusers provides approximate balancing of intensity between cameras (Girard 2001).

The second system using of a portable high stability xenon flash lamp. The Roving Xenon Flasher (RXF) provides a standard candle that can be moved from camera to camera, site to site, and from controlled laboratory conditions to the harsh environment in the field. The RXF offers several advantages. The pulse-to-pulse variation in intensity is very small  $\sim 0.3\%$  and the stability over a night is better than 2%. The emission spectrum of the RXF is sufficiently broad to allow calibration at various wavelengths. NIST traceable reference detectors are used to measure the absolute output of the RXF under controlled conditions. The RXF is then used to determine the absolute response of the PMTs. In addition to the original NIST calibrated standard detectors, (Bird 1994) several new NIST traceable detectors are being developed and tested for the purpose of independently verifying the absolute scale of the calibration. The main drawback of this system is that it is very time consuming and labor intensive.

### 3 Gain Measurement

The first step in the calibration of a PMT is the measurement of the average number of photoelectrons. The ratio of the output charge to the number of photoelectrons (i.e. electronic gain) is independent of the choice of light source. Measurements employing various sources of light, such as blue or UV LED's, Xenon flashers, lasers, etc. can, therefore, be directly compared. The mean number of photoelectrons is estimated from the shape of the measured charge distribution (RCA) (Bellamy 1994) (Abu-Zayyad 1997).

$$\begin{aligned}\mu &= G \cdot pe \\ \sigma &= G\sqrt{\alpha} \cdot \sqrt{pe}\end{aligned}$$

Here  $\mu$  and  $\sigma$  are the mean and standard deviation of the charge distribution,  $G$  is the electronic gain of the PMT,  $pe$  is the mean number of photoelectrons, and  $\sqrt{\alpha}$  is the PMT excess noise factor. The number of photoelectrons is computed

using the following formula:

$$N_{pe} = \frac{(n-3)}{(n-1)} \cdot \alpha \frac{\bar{Q}^2}{S^2} - \frac{\alpha}{n}, \quad n > 3 \quad (3.1a)$$

$N_{pe}$  is the estimate for  $pe$ ,  $n$  is the number of measurements,  $\bar{Q}$  is the mean of the charge distribution, and  $S$  is the standard deviation. If the number of photoelectrons and the number of measurements are large enough this formula approaches the more familiar expression:

$$N_{pe} \approx \alpha \frac{\bar{Q}^2}{S^2}, \quad n \gg 3 \quad (3.1b)$$

The statistical error for the estimate is given by:

$$\sigma_{N_{pe}}^2 = \frac{2}{(n-5)} pe^2 \left[ 1 + 2(n-2) \left( \frac{\alpha}{n \cdot pe} \right) + (n-2) \left( \frac{\alpha}{n \cdot pe} \right)^2 \right], \quad n > 5 \quad (3.2a)$$

This expression simplifies when the number of measurements and number of photoelectrons are sufficiently large:

$$\sigma_{N_{pe}}^2 \approx \frac{2}{(n-5)} pe^2, \quad n \gg 5 \quad (3.2b)$$

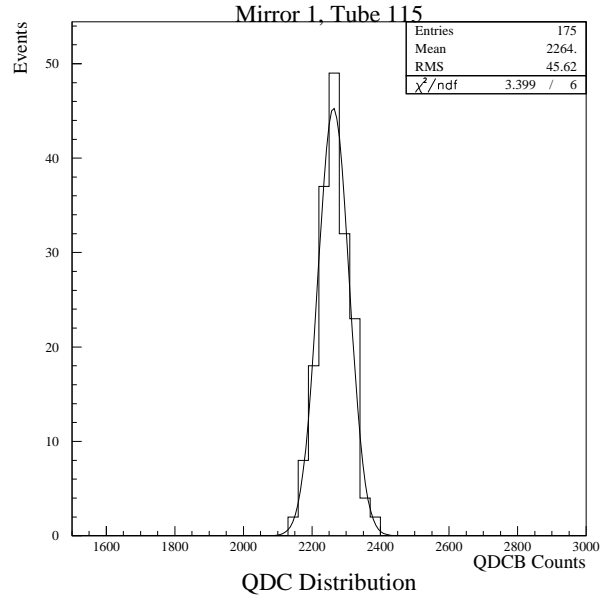
The true value of  $\sqrt{\alpha}$  is not directly measured but is included as a component of the measured parameters.

Figure 1 shows the measured charge distribution for a single HiRes PMT channel. An estimate of  $3726 \pm 404$  photoelectrons was computed for this measurement. The uncertainty in the estimated number of photoelectrons is larger because it contains uncertainties from both the mean and standard deviation of the charge distribution.

Fluctuations in the light source has the effect of increasing  $S$  in equation (3.1a) for  $N_{pe}$  causing the photoelectron estimate to be reduced. This causes corresponding errors to increase when the calibration is applied. That is, the errors in the resulting photon numbers will be overestimated.

In HiRes, each camera consists of 256 PMTs that independently and simultaneously measure each flash. Normalizing the individual charge measurements by the average response of the entire camera effectively reduces the fluctuations due to the source by a factor of  $\sqrt{256}$ . The efficacy of this technique of normalizing measurements has been verified by simulation and also by comparing the measurements made using the highly stable RXF and those made using the less stable YAG/fiber system.

During an RXF calibration, several pulse intensities are achieved through the use of neutral-density filters. Figure 2 shows the response of a typical PMT to four different intensities. The mean pedestal subtracted response of the system to a sequence of shots is plotted in the vertical direction, where the horizontal axis represents the mean number of photoelectrons estimated using equation (3.1b). These points clearly fit well to a straight line through the origin as expected. The gain of the PMT channel is the fitted slope. Also shown in figure 2 is a point corresponding to the YAG laser calibration



**Fig. 1.** The measured charge (QDC) distribution for a single HiRes PMT. The parameters of the charge distribution are used to estimate the number of photoelectrons.

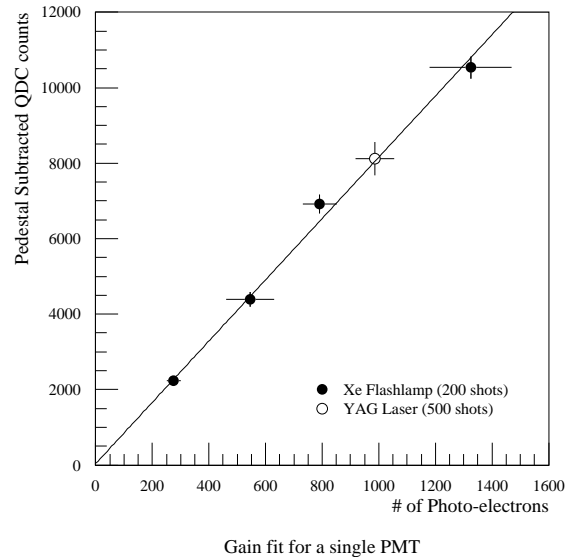


**Fig. 2.** Calibration data, including both RXF and YAG/fiber system measurements, for a typical tube at HiRes-I.

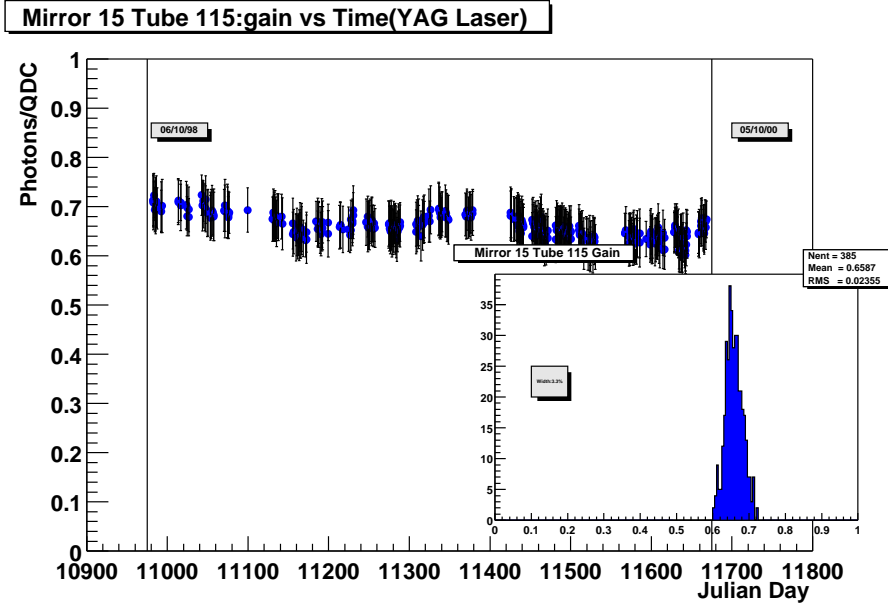


**Fig. 3.** HiRes-I mirror 15 channel 115 gain as recorded over a two year period.

taken during the same night. The YAG data ( $\sim 500$  samples) is analyzed in precisely the same manner as the RXF data ( $\sim 200$  samples at each intensity). The measurements are clearly in excellent agreement. Photoelectron error bars shown in the plot represent a robust statistical error estimation using the Bootstrap numerical method.

#### 4 Detector Stability

The technique described here has been used to track the gains of the detectors in the HiRes-I experiment over a period of three years. Figure 4 shows the system wide variation in gain over this period plotted as a function of day of the year. The ratio of each PMT's gain to it's average gain over the entire period is then averaged over all PMTs in the experiment to provide a single point. The change consists primarily of a  $\sim 5\%$  seasonal variation. The gain variation is probably related to the seasonal variation in temperature. However, it is difficult to directly correlate the changes with temperature because the temperatures of individual system components do not vary simply with the external temperature. In the figure the RXF measurements are superimposed on the measurements made using the YAG/fiber system. The error bars represent the spread of the individual PMTs in the detector. The plot clearly demonstrates the excellent agreement between the two measurements.

Figure 3 shows the gain for an example PMT. Individual PMTs show the same seasonal variation seen for the entire detector.

Figure 5 shows the relative change in gain of PMTs over a night. The plot contains data for all PMTs in the HiRes-I detector over the three year period. This change is much less than that over one year,  $\sim 2\%$ , and is based on the nightly YAG/fiber measurements. Although the gains of the PMT's

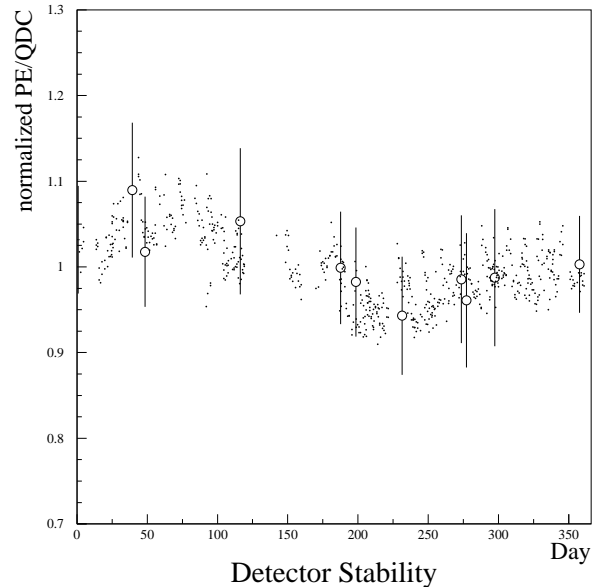
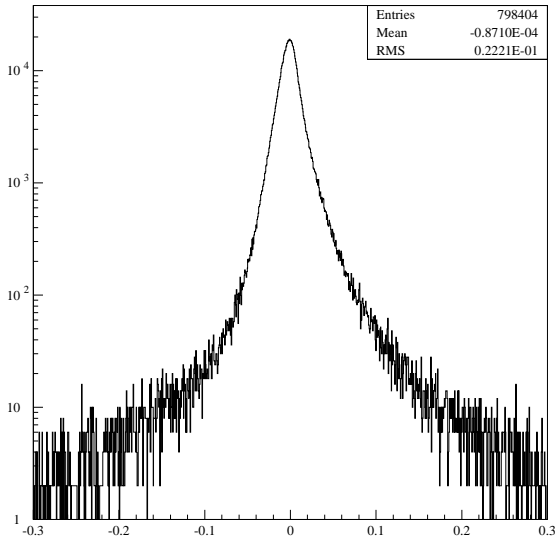


**Fig. 4.** Three years of HiRes-I relative gain measurements plotted vs Julian day modulo  $365\frac{1}{4}$ . Nightly YAG/fiber measurements are shown as solid dots, while the open circles represent measurements using the RXF.

exhibit noticeable variation over time, these changes are routinely monitored at the level of a few percent.

#### 5 Discussion

The method of calibrating the HiRes PMTs using the statistics of the measured charge distributions works well. Once sources of systematic error such as operator error, equipment



Change in Detector Response From Beginning to End of Night

**Fig. 5.** Nightly relative change in gain for all PMTs in HiRes-I over a two year period.

failures, etc. have been eliminated the results are consistent with the predicted errors.

New NIST traceable standard detectors are being developed independently at collaborating institutions to provide redundant verification of the absolute scale of the calibration. Along with the new standard detectors, the use of narrow band sources, or of narrow band filters in conjunction with the RXF, will, in particular, allow testing of the basic assumptions regarding the system. For instance, the wavelength dependence of PMT quantum efficiency can be measured for every PMT.

Finally, the expressions for the statistically unbiased photoelectron estimator (3.1a) and for the associated statistical error (3.2a) should be useful to other researchers who seek to employ similar techniques.

## 6 Acknowledgments

This work is supported in part by the National Science Foundation (grants PHY-93-22298, PHY-99-74537, & PHY-99-04048) and by the U.S. Department of Energy (grant FG03-92ER40732) and by the Australian Research Council. We gratefully acknowledge the contributions from the technical staffs of our home institutions. We would like to thank Colonels John Como and Edward Fisher as well as the staff of Dugway Proving Grounds for their continued cooperation and assistance. We would also like to thank the University of Utah's Center for High Performance Computing for their support.

## References

- J.H.V. Girard *et al.*, *A fiber-optic-based calibration system for the High Resolution Fly's Eye cosmic ray observatory*, *Nucl. Instr. and Meth. A* 460, (2001) pg. 278.
- D. Bird *et al.*, *The Calibration of the Absolute Sensitivity of Photomultiplier Tubes in the High Resolution Fly's Eye Detector*, *Nucl. Instr. and Meth. A* 319, (1994) pg. 592.
- RCA Photomultiplier Handbook, Statistical Theory of Noise in Photomultiplier Tubes*, Appendix G, pg. 160.
- E.H. Bellamy *et al.*, *Absolute Calibration and Monitoring of a Spectrometric Channel Using a Photomultiplier*, *Nucl. Instr. and Meth. A* 339, (1994) pg. 468.
- T. Abu-Zayyad *et al.*, *Calibration and stability measurements of a FADC based data acquisition system for the HiRes Fly's Eye experiment*, *25th ICRC (Durban, South Africa)* 7, (1997) pg. 213 (HE 6.1.5)
- A.G. Wright, *A Monte Carlo Simulation of Photomultiplier Resolution*, *IEEE Trans. Nucl. Sci. NS-34*, No. 1, (1987) pg. 414.